The Abdus Salam International Centre for Theoretical Physics

United Nations Educational, Scientific and Cultural Organization

IAEA International Atomic Energy Agency

2065-36

Advanced Training Course on FPGA Design and VHDL for Hardware Simulation and Synthesis

26 October - 20 November, 2009

Three-dimensional deconvolution in FPGA

Fabio Mammano
University of Padua
Faculty of Medicine and Surgery
Department of Physics
via Marzolo 8
35131 Padova
Italy

Three-dimensional deconvolution in FPGA

Summary of deconvolution

Deconvolution **is a computationally intensive image processing technique that is being increasingly utilized for improving the contrast and resolution of digital images captured in the microscope. The foundations are based upon a suite of methods that are designed to remove or reverse the blurring present in microscope images induced by diffraction.**

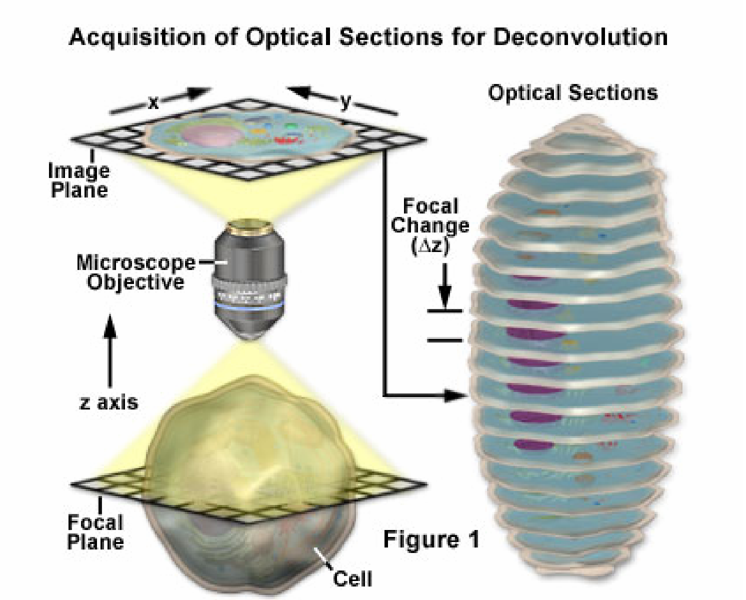

The basic concepts surrounding acquisition of serial optical sections for deconvolution analysis are presented with a schematic diagram in Figure 1.

- **The specimen is an idealized cell from which a series of optical sections are recorded along the z-axis of an optical microscope.**
- **For each focal plane in the specimen, a corresponding image plane is recorded by the detector and subsequently stored in a data analysis computer.**
- **During deconvolution analysis, the entire series of optical sections is analyzed to create a three-dimensional montage.**

Modeling the effect of an optical system: 3D input-output relationship

$i(x, y, z)$: **Input light distribution**

$s(x, y, z)$: **Impulse response (3D PSF): describes a process causing the output distribution to be different from the original scene.**

$o(x, y, z)$: **Output light distribution**

Model equation:

$$\boxed{o(x, y, z) = i(x, y, z) \otimes s(x, y, z)}$$

The 3D convolution operation is defined as:

$$o(x, y, z) = \iiint_{u,v,w} i(u, v, w)\, s(x-u, y-v, z-w)\, du \quad dv \quad dw$$

The impulse response (3D PSF), is the output light distribution in image space for a point source input in object space.

Z-stack decomposition

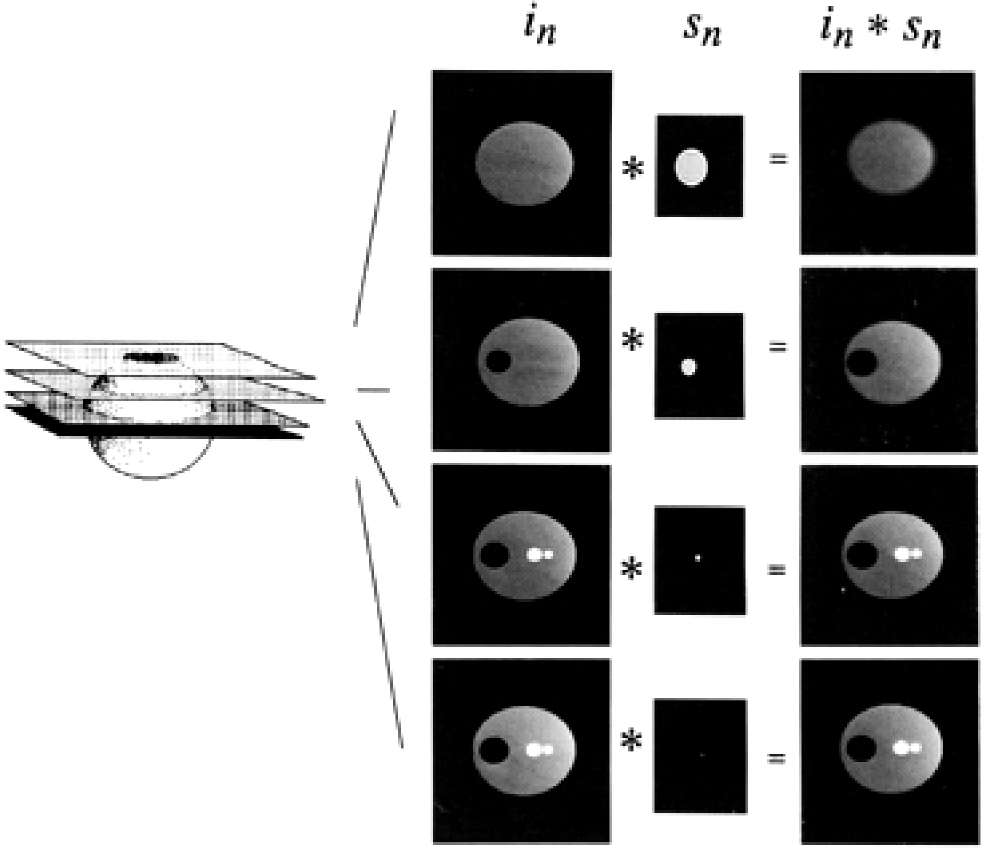

We can start by trying to decompose the 3D model equation

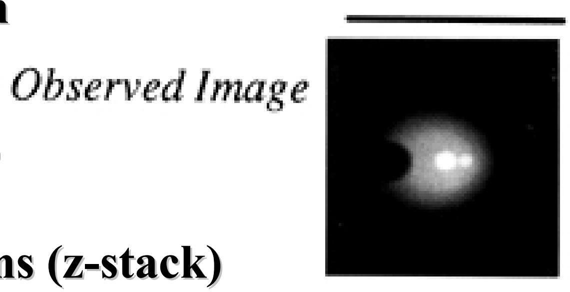

$$o(x, y, z) = i(x, y, z) \otimes s(x, y, z)$$

into a set of through-focus two-dimensional series expansions (z-stack)

$$\boxed{o_z(x, y) = i_0(x, y) \otimes s_0(x, y) + i_{-1}(x, y) \otimes s_{-1}(x, y) + i_{+1}(x, y) \otimes s_{+1}(x, y) + \ldots}$$

Function $s_k(x,y)$, $k = -N,\ -N+1 \ldots,\ 0,\ 1,\ 2\ \ldots N$, are sections through the 3-D PSF taken in planes orthogonal to the optic axis of the system

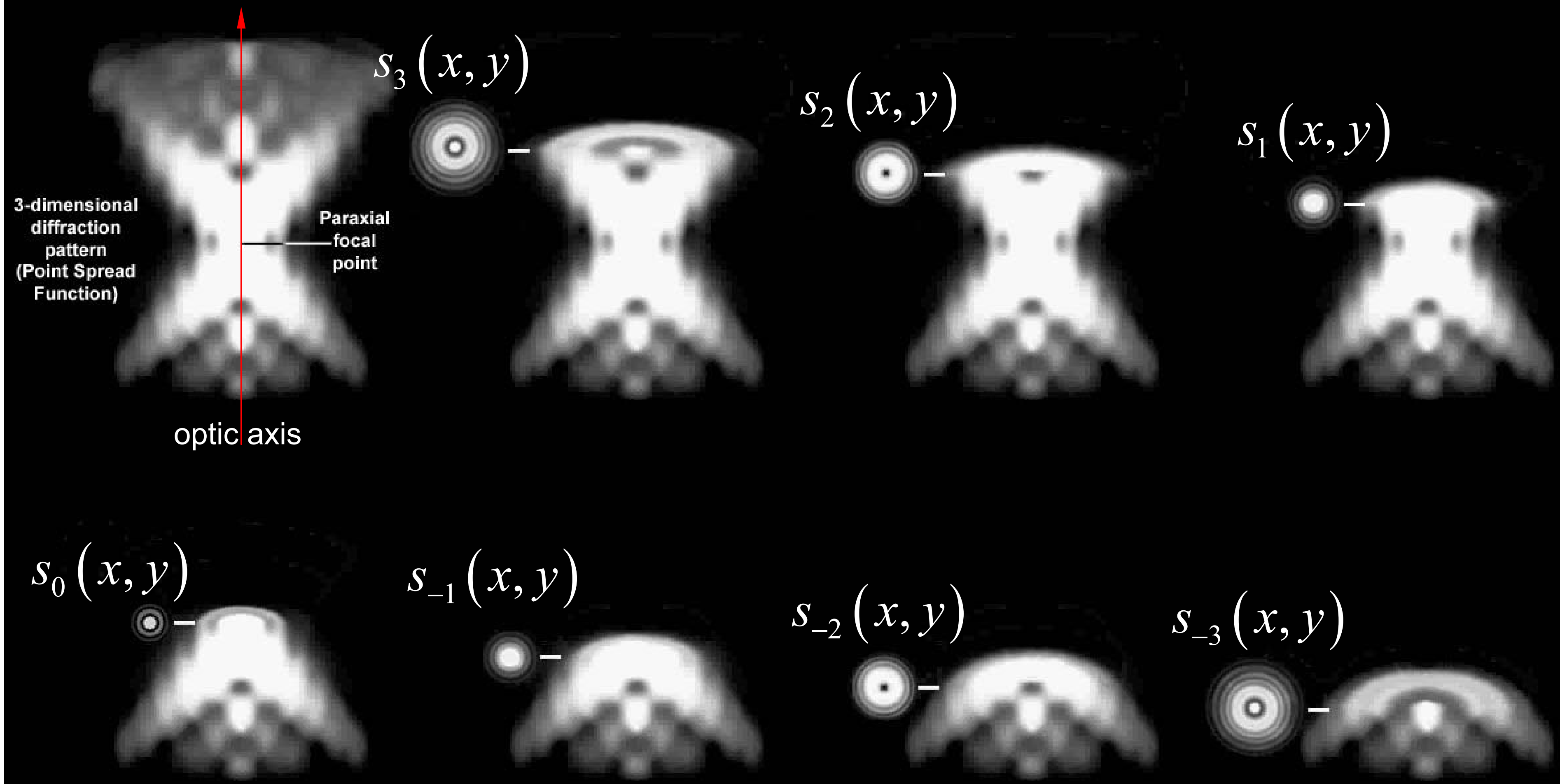

$$\boxed{o_z(x,y) = i_0(x,y) \otimes s_0(x,y) + i_{-1}(x,y) \otimes s_{-1}(x,y) + i_{+1}(x,y) \otimes s_{+1}(x,y) + \ldots}$$

To convert these equations into an algorithm that can be used in practice, we will make two simplifying assumptions:

1. **Out-of-focus light contribution other than those from the <u>adjacent planes</u> are negligible, i.e. terms with index different from 0 or ±1 can be ignored:**

$$o_z(x,y) \cong i_0(x,y) \otimes s_0(x,y) + \\ + i_{-1}(x,y) \otimes s_{-1}(x,y) + \\ + i_{+1}(x,y) \otimes s_{+1}(x,y)$$

(this assumption is not strictly necessary and will be relaxed later).

2. **Light originating from planes immediately above or below the plane of focus can be approximated by images taken while focusing on these planes, i.e.**

$$i_{-1} \cong o_{-1}$$

$$i_{+1} \cong o_{+1}$$

(Castelman, 1979)

Z-stack decomposition

Taking plane $z=0$ as the reference focal plane,

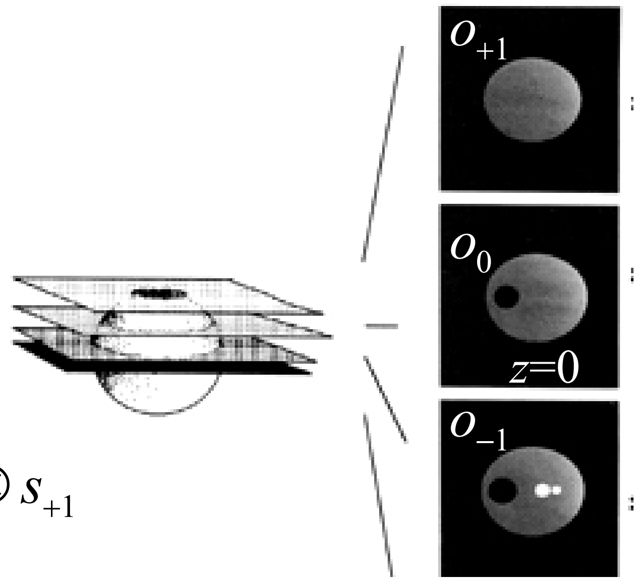

we write the simplified equation

$$o_0 = i_0 \otimes s_0 + o_{-1} \otimes s_{-1} + o_{+1} \otimes s_{+1}$$

in the form

$$i_0 \otimes s_0 = o_0 - o_{-1} \otimes s_{-1} - o_{+1} \otimes s_{+1}$$

Now we take the Fourier transform, F, of both sides:

$$F\left(i_0 \otimes s_0\right) = F\left(o_0 - o_{-1} \otimes s_{-1} - o_{+1} \otimes s_{+1}\right)$$

By applying the convolution theorem we obtain

$$F\left(i_0\right) \cdot F\left(s_0\right) = F\left(o_0 - o_{-1} \otimes s_{-1} - o_{+1} \otimes s_{+1}\right)$$

and therefore

$$F\left(i_0\right) = F\left(o_0 - o_{-1} \otimes s_{-1} - o_{+1} \otimes s_{+1}\right) \cdot \frac{1}{F\left(s_0\right)}$$

Taking the inverse Fourier transform, F^{-1}, of both sides finally yields:

$$i_0 = F^{-1}\left[F\left(o_0 - o_{-1} \otimes s_{-1} - o_{+1} \otimes s_{+1}\right) \cdot \frac{1}{F\left(s_0\right)}\right]$$

Nearest neighbor (NN) deconvolution

With the stated assumptions, the in-focus light distribution i_o can be recovered (restored) from the equation:

$$i_0 = \left(o_0 - o_{-1} \otimes s_{-1} - o_{+1} \otimes s_{+1}\right) \otimes F^{-1}\left(\frac{1}{F\left(s_0\right)}\right)$$

<u>In practice</u>, nearest neighbor deconvolution is performed using a modified form of the above equation:

$$\boxed{i_0 = \left(o_0 - c_{-1} o_{-1} \otimes s_{-1} - c_{+1} o_{+1} \otimes s_{+1}\right) \otimes F^{-1}\left(\frac{F^*\left(s_0\right)}{\left|F\left(s_0\right)\right|^2 + c_0}\right)}$$

where c_{-1} , c_{+1} and c_0 are empirical factors and all PSFs are normalized.

Coefficients $c_{\pm 1}$ are used to limit errors caused by over-compensating out-of-focus contributions and their value falls generally in the range from 0.01 to 0.1.

$$F^{-1}\left(\frac{F^*(s_0)}{\left|F(s_0)\right|^2 + c_0}\right)$$

usually complex ≈ 0.045

c_0 is required to handle exceptions caused by the possible presence of zeros in $F(s_0)$; values for c_0 fall in the range from 0.045 to 0.050. Note that:

- **Too large a value for c_0 causes loss of details and yields blurry images.**
- **Too small a value causes amplification of random noise into bright spots, rings, or patches.**

Multi-neighbour deconvolution

Relaxing condition 1 and generalizing to N neighbours yields the result:

$$i_0 = \left(o_0 - \sum_{j=1}^{N} \left(c_{-j} o_{-j} \otimes s_{-j} + c_{+j} o_{+j} \otimes s_{+j} \right) \right) \otimes F^{-1} \left(\frac{F^*(s_0)}{\left| F(s_0) \right|^2 + c_0} \right)$$

In summary, this procedure requires:

- **in focus and out-of-focus image collection**
- **in focus and out-of-focus PSF measurement**

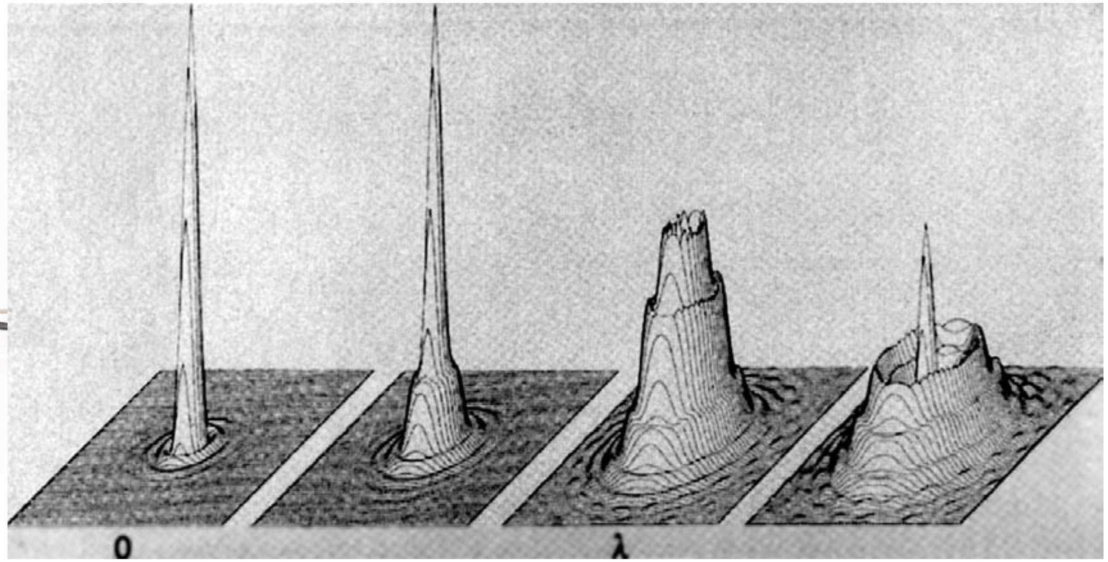

Through-focus behaviour of point images

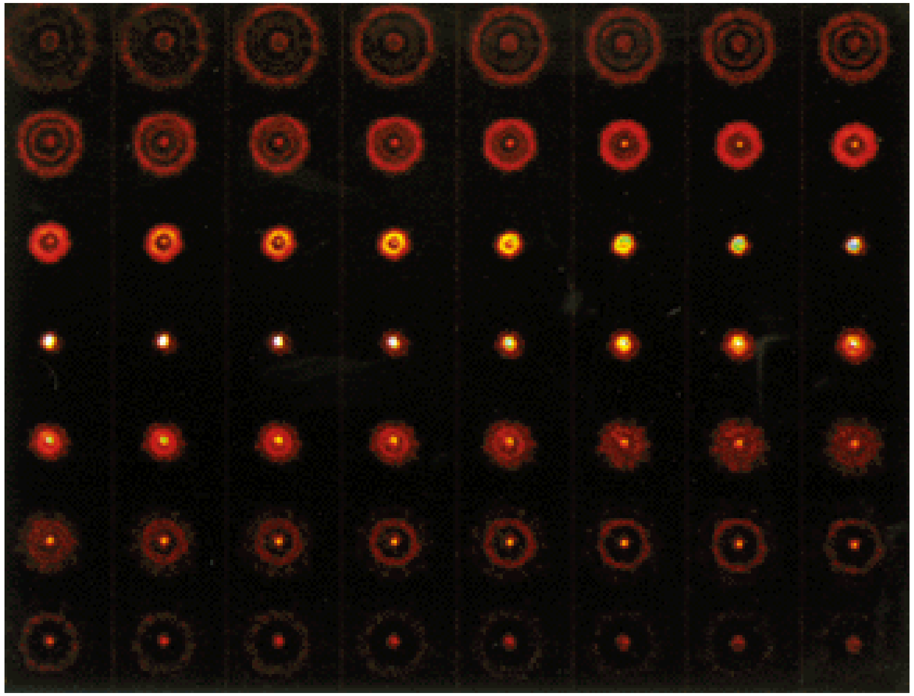

Serial focal sequence of fluorescence images of a 200 nm bead used to measure *x-y* sections of the 3D PSF at various distances above and below the focal plane

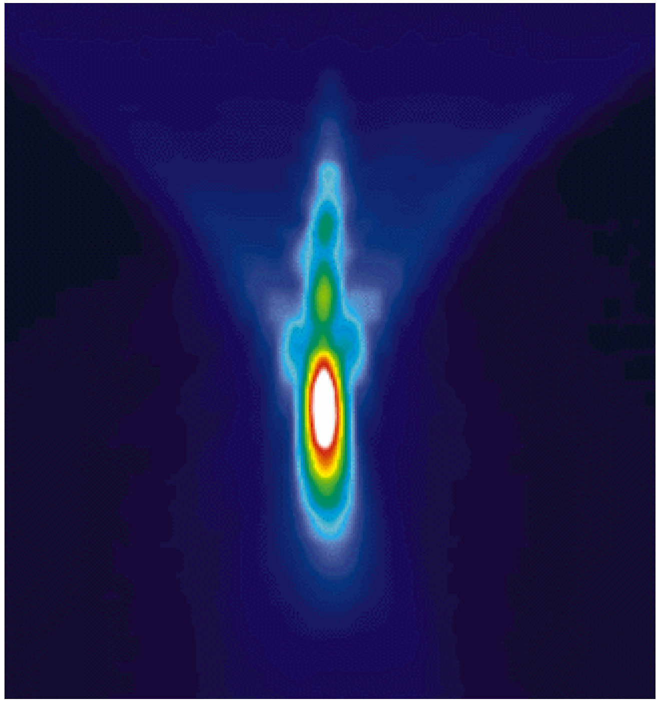

Meridional (*y-z*) section through the PSF. This pseudo-color image was generated electronically from the series of bead images shown at left.

The asymmetry in the axial direction is due to spherical aberration and is very common in imaging biological specimens. There is additional path length through a layer of water, glycerol or other mounting medium, which leads to increased spherical aberration.

Measuring the 3D PSF

The 3D PSF must be measured on the same system used to acquire the images to be deconvolved. For fluorescence imaging, this process requires:

- **Embedding sub-resolution fluorescent beads into the medium of interest. If this is cytoplasm, the beads can be incorporated by cell *electroporation*.**
- **Setting the step of the *z*-stack: Nyquist theorem.**
- **Finding the (closest approximation to) the focal plane; by definition, this is the plane where the lateral extent of the PSF is minimal and its peak value is maximal**
- **Symmetrization: in the absence of aberrations, the PSF has rotational symmetry around the optical axis; raw *x-y* PSF sections are made symmetric by a circular averaging procedure.**
- **Normalization: in an ideal widefield microscope, the total integrated intensity at each out-of-focus plane is constant.**

A typical 11×11 kernel

32	51	51	51	51	50	50	51	51	50	33
52	80	81	79	79	80	80	81	80	81	51
51	80	79	81	82	81	81	81	80	80	51
50	81	80	82	86	87	84	82	81	81	52
52	82	83	85	104	154	103	84	82	81	52
52	83	82	88	116	395	148	87	82	81	52
51	82	83	85	98	116	102	86	80	81	52
52	81	82	84	85	84	83	83	81	82	52
52	82	81	81	82	82	82	82	82	82	51
51	80	81	82	80	81	82	81	82	82	52
33	50	51	51	51	51	50	51	51	52	33

Algorithm validation: optical sections of a 15 μm test sphere

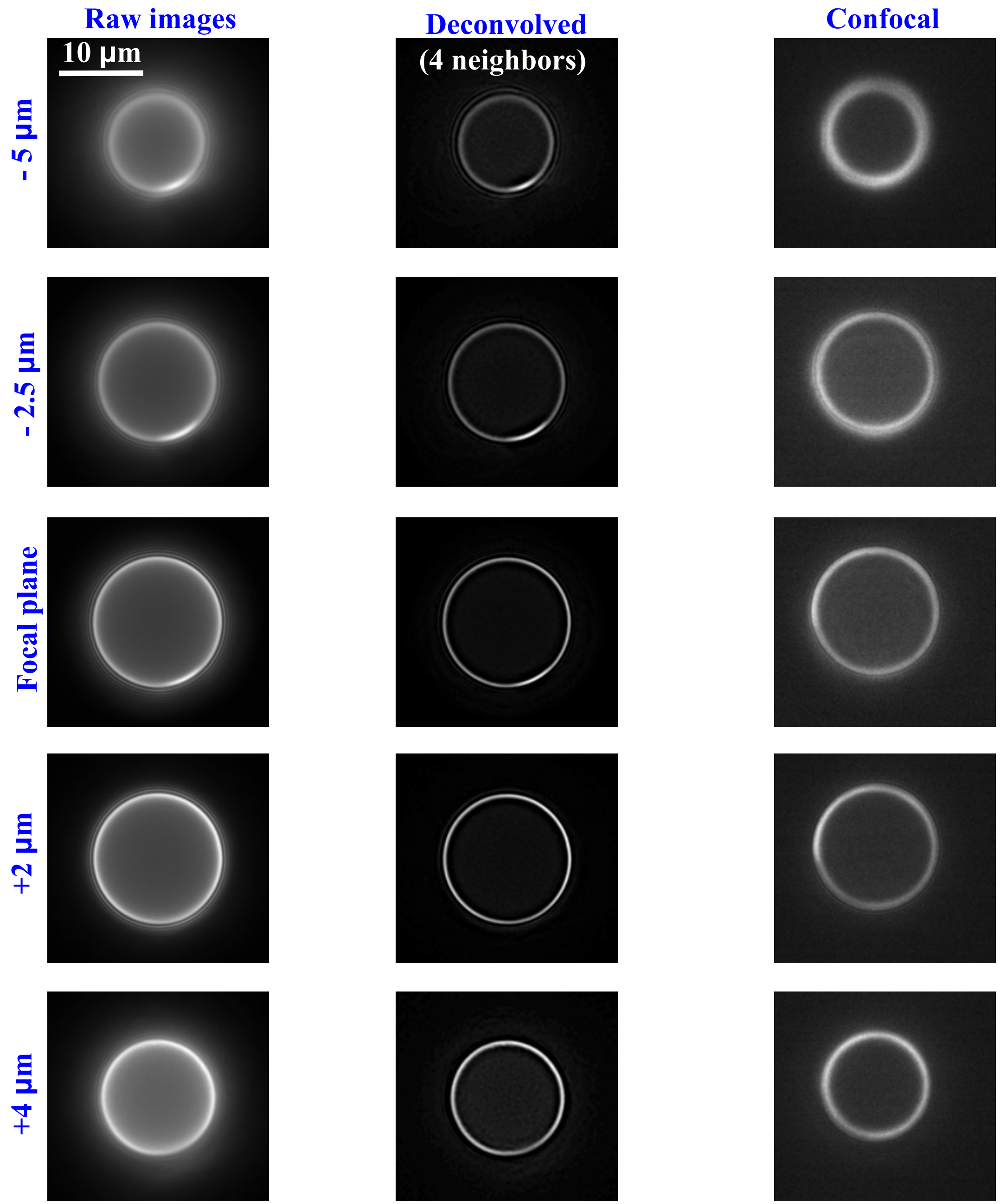

Application to biological specimens

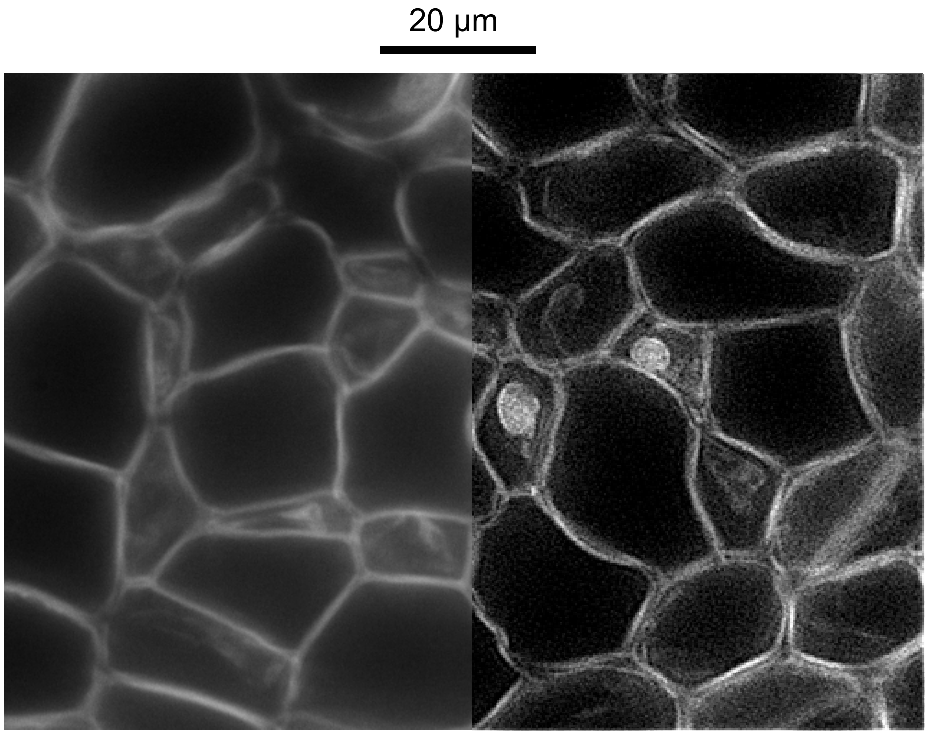

Conventional (wide-field) fluorescence image of Convallaria Rhizom (*left*), deconvolved with the nearest neighbour algorithm (*right*).

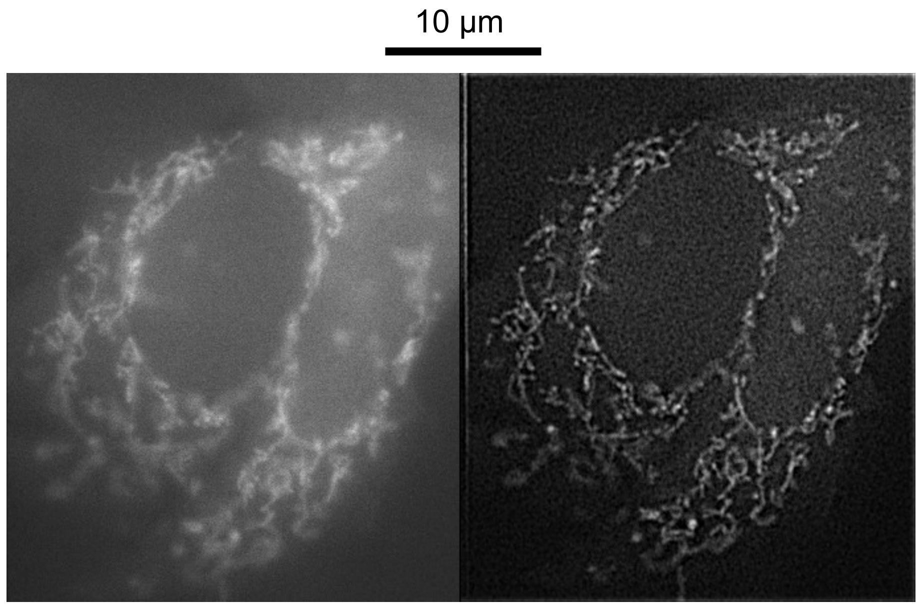

Z-stack of mitochondria targeted with cameleon

NN deconvolution in real time: FPGA

One deconvolved image requires 3 consecutive images. However, the last one of a frame triplet is also the first one of the following triplet. Therefore deconvolved frames are generate at half the acquisition frame rate.

CCD camera target frame rate:

60 frames per second (fps), to obtain 30 fps of NN deconvolved images

CCD size:

512 × 512 pixels (binnig = 2×2 on a Mpixel sensor)

Reasonable kernel size:

11 × 11 pixels

Number of multiplications (and additions) per frame:

$$(512 \times 512) \times (11 \times 11) = 31.7 \text{ M}$$

At 60 fps:

$$31.7 \text{ M} \times 60/\text{s} = 1.9 \text{ G/s}$$

Computational parallelism is a must!

Breaking down the problem into time slots

$$i_0 = \left(o_0 - c_{-1} o_{-1} \otimes s_{-1} - c_{+1} o_{+1} \otimes s_{+1}\right) \otimes F^{-1}\left(\frac{F^*(s_0)}{\left|F(s_0)\right|^2 + c_0}\right)$$

constant scalar *constant matrix*

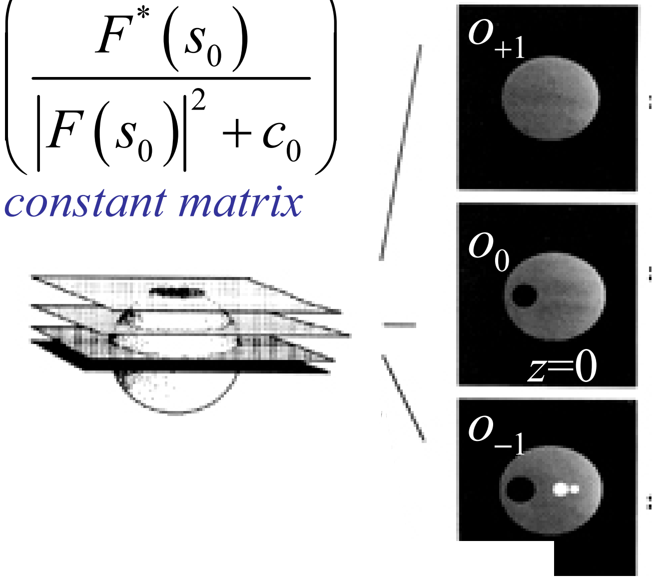

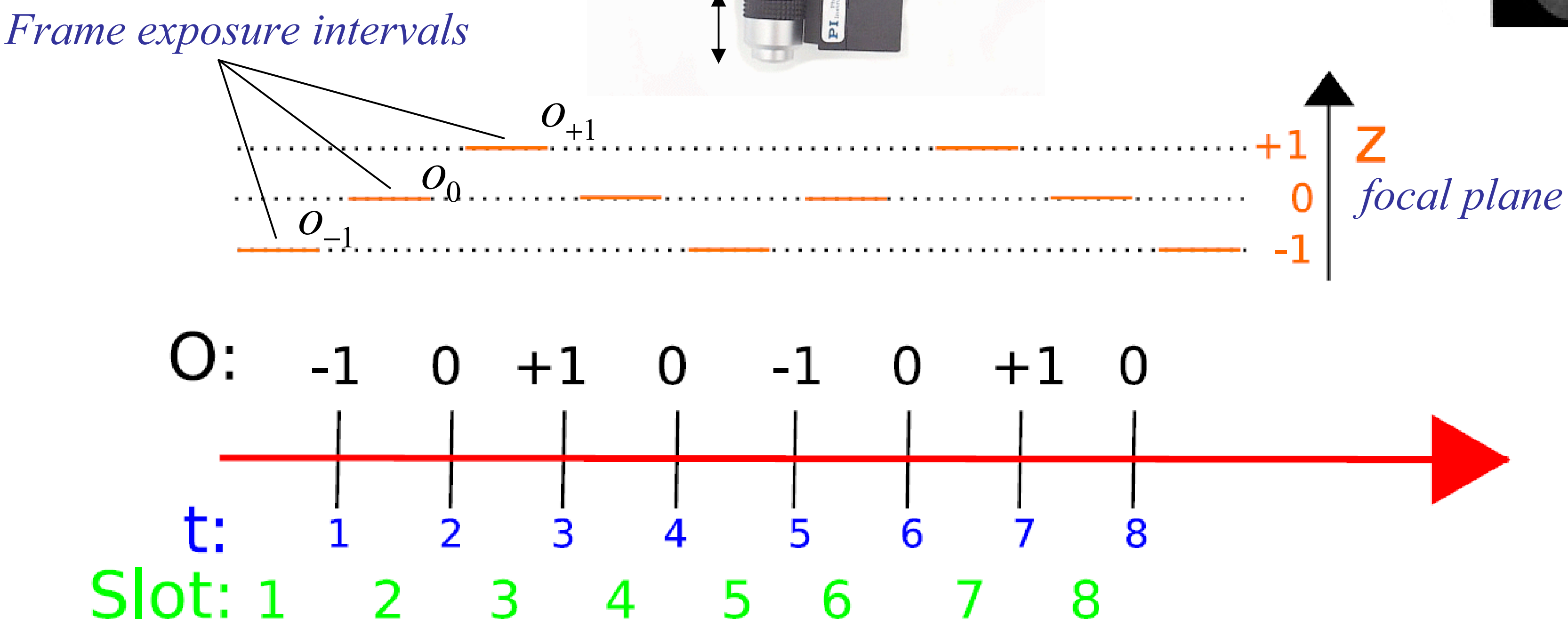

Overview of Slots 1, 2 and 3

- **Slot 1: collect light to form image** o_{-1}
- **Slot 2: download image** o_{-1} **data while collecting light to from image** o_0
- **Slot 3: download image** o_0 **data while collecting light to form image** o_{+1}
- ....

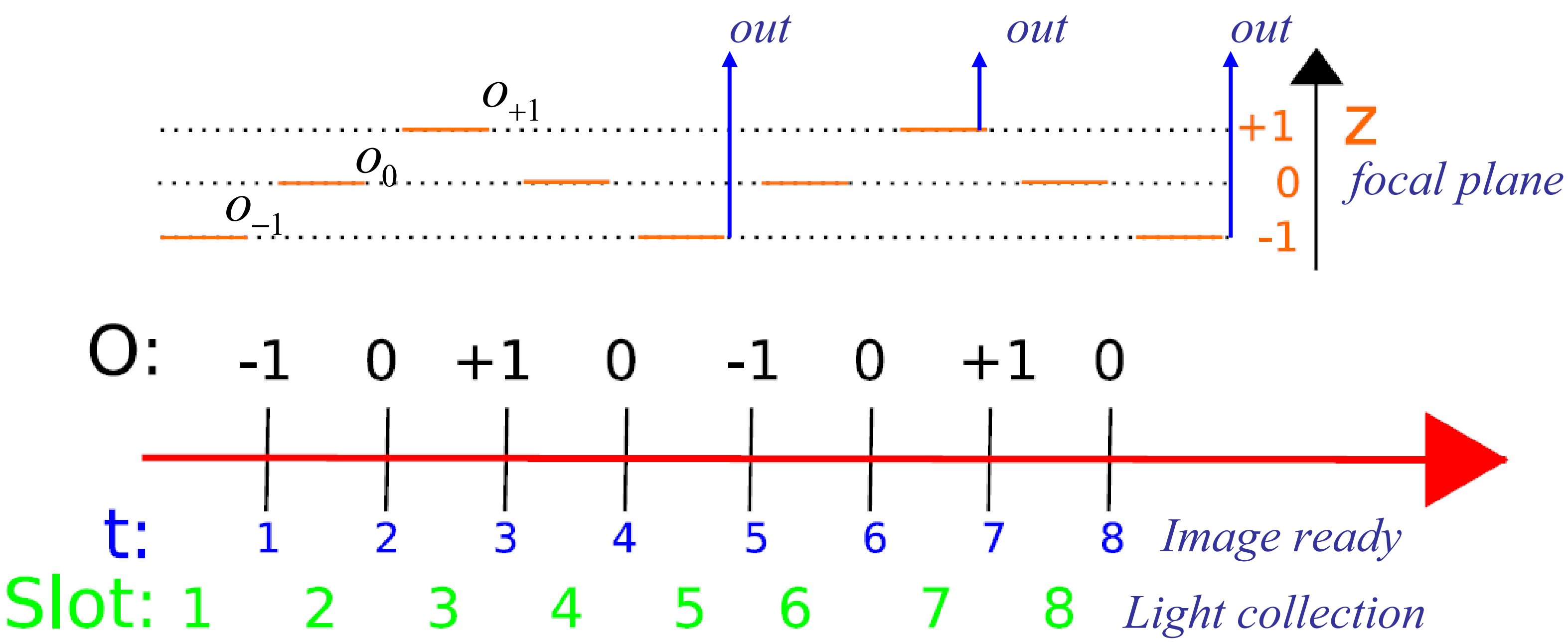

Slot 2 in detail

$$i_0 = \left(o_0 - \underbrace{c_{-1} o_{-1} \otimes s_{-1}}_{i_{-1}} - c_{+1} o_{+1} \otimes s_{+1} \right) \otimes F^{-1} \left(\frac{F^*(s_0)}{|F(s_0)|^2 + c_0} \right)$$

- Collect light to form image o_0;
- in parallel, as o_{-1} data come through, compute

$$\boxed{i_{-1} = c_{-1} o_{-1} \otimes s_{-1}}$$

- store the result into a memory buffer.

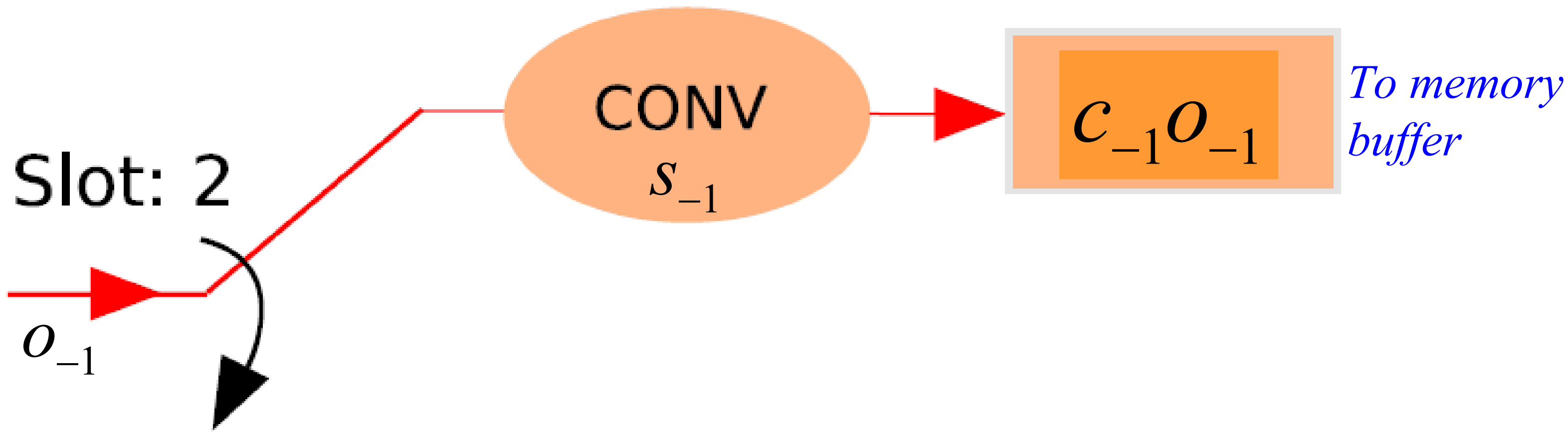

Slot 3 in detail

$$i_0 = \left(o_0 - \underbrace{c_{-1} o_{-1} \otimes s_{-1}}_{i_{-1}} - c_{+1} o_{+1} \otimes s_{+1} \right) \otimes F^{-1} \left(\frac{F^*(s_0)}{\left|F(s_0)\right|^2 + c_0} \right)$$

Computed in Slot 2

- **collect light to form image o_{+1} ;**
- **in parallel, as o_0 data come through, subtract the result (i_{-1}) obtained in Slot 2;**
- **store also this new result into a memory buffer.**

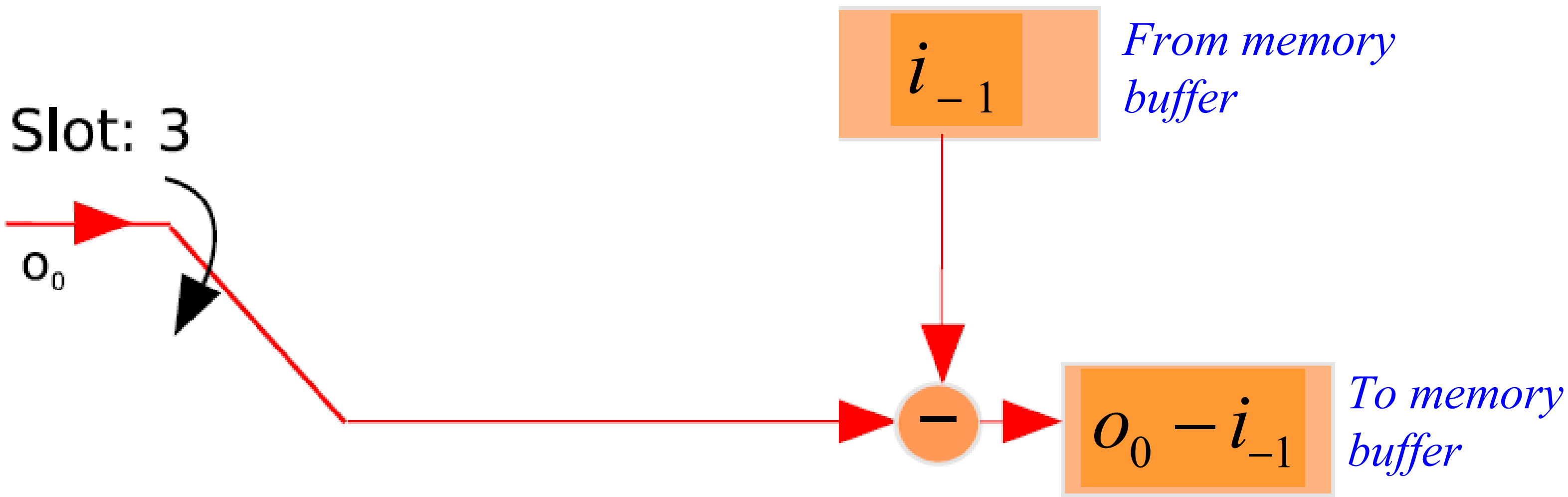

Slot 4 in detail

$$i_0 = \left(o - c_{-1}o_{-1} \otimes s_{-1} - \underbrace{c_{+1}o_{+1} \otimes s_{+1}}_{i_{+1}} \right) \otimes F^{-1}\left(\frac{F^*(s_0)}{\left|F(s_0)\right|^2 + c_0} \right)$$

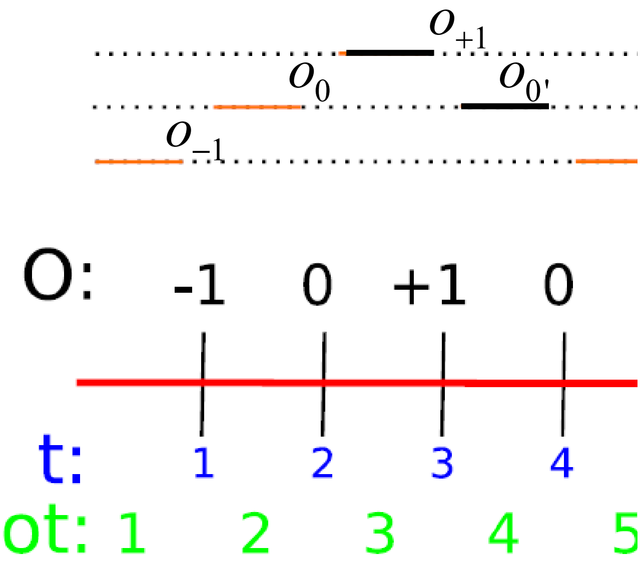

- **collect light to form a new image $o_{0'}$;**
- **as o_{+1} data from Slot 3 come through compute:**

$$\boxed{i_{+1} = c_{+1}o_{+1} \otimes s_{+1}}$$

- **subtract this new result from the partial difference ($o_0 - i_{-1}$) obtained in Slot 3.**

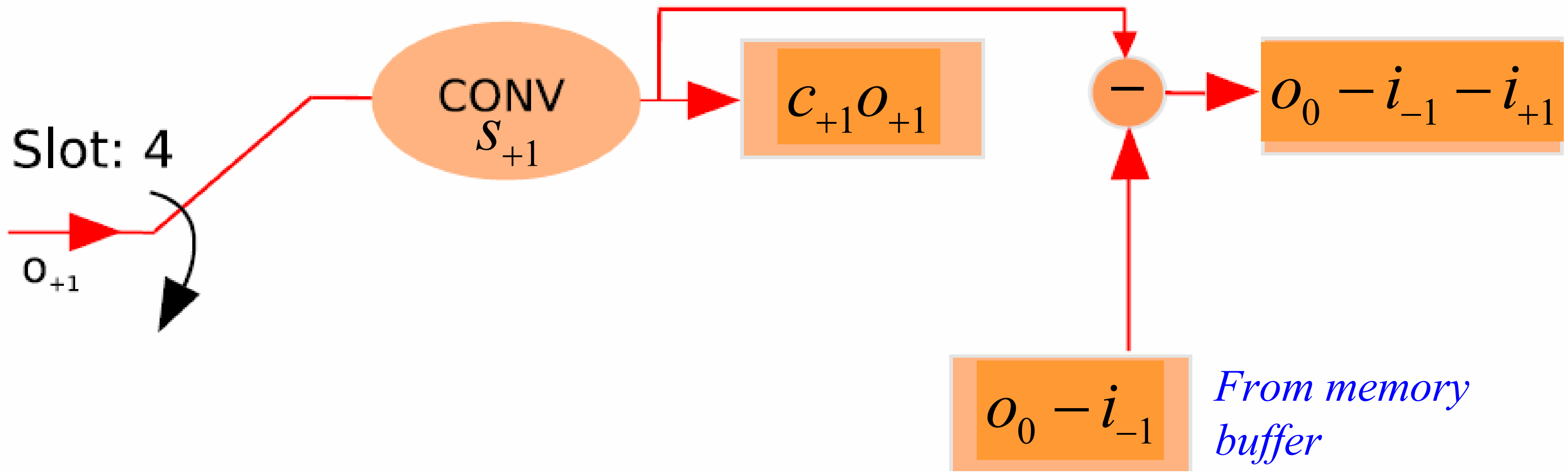

Slots 5 in detail

$$i_0 = \underbrace{\left(o - c_{-1} o_{-1} \otimes s_{-1} - c_{+1} o_{+1} \otimes s_{+1}\right)}_{\textit{Computed in Slot 4}} \otimes F^{-1}\left(\frac{F^*\left(s_0\right)}{\left|F\left(s_0\right)\right|^2 + c_0}\right)$$

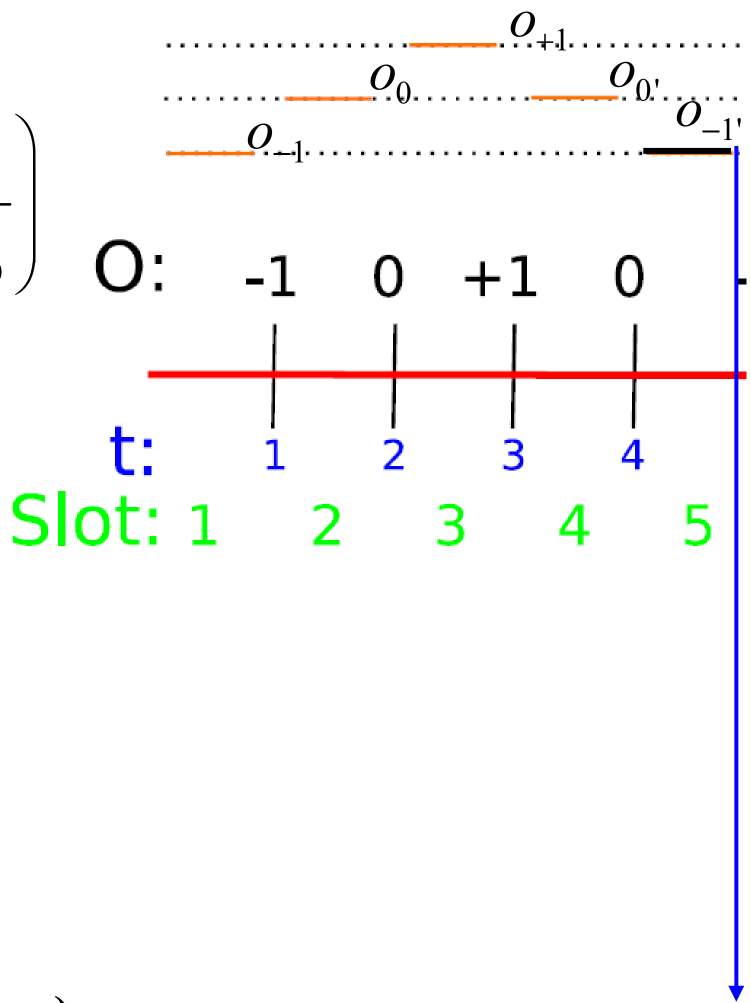

- **collect light to form a new image $o_{-1'}$**
- **in parallel, convolve the result of Slot 4, that is**

$$o_0 - i_{-1} - i_{+1}$$

with matrix

$$F^{-1}\left(\frac{F^*\left(s_0\right)}{\left|F\left(s_0\right)\right|^2 + c_0}\right)$$

(which must have been previously stored in memory)

- **the results is the <u>first deconvolved image</u>, which is sent to the host PC**

FPGA example: convolution with a separable kernel

$$s(j,k) = s_1(j)s_2(k)$$

$$o(m,n) = \sum_{k=1}^{N_2} s_2(n-k) \sum_{j=1}^{N_1} i(j,k)s_1(m-j)$$

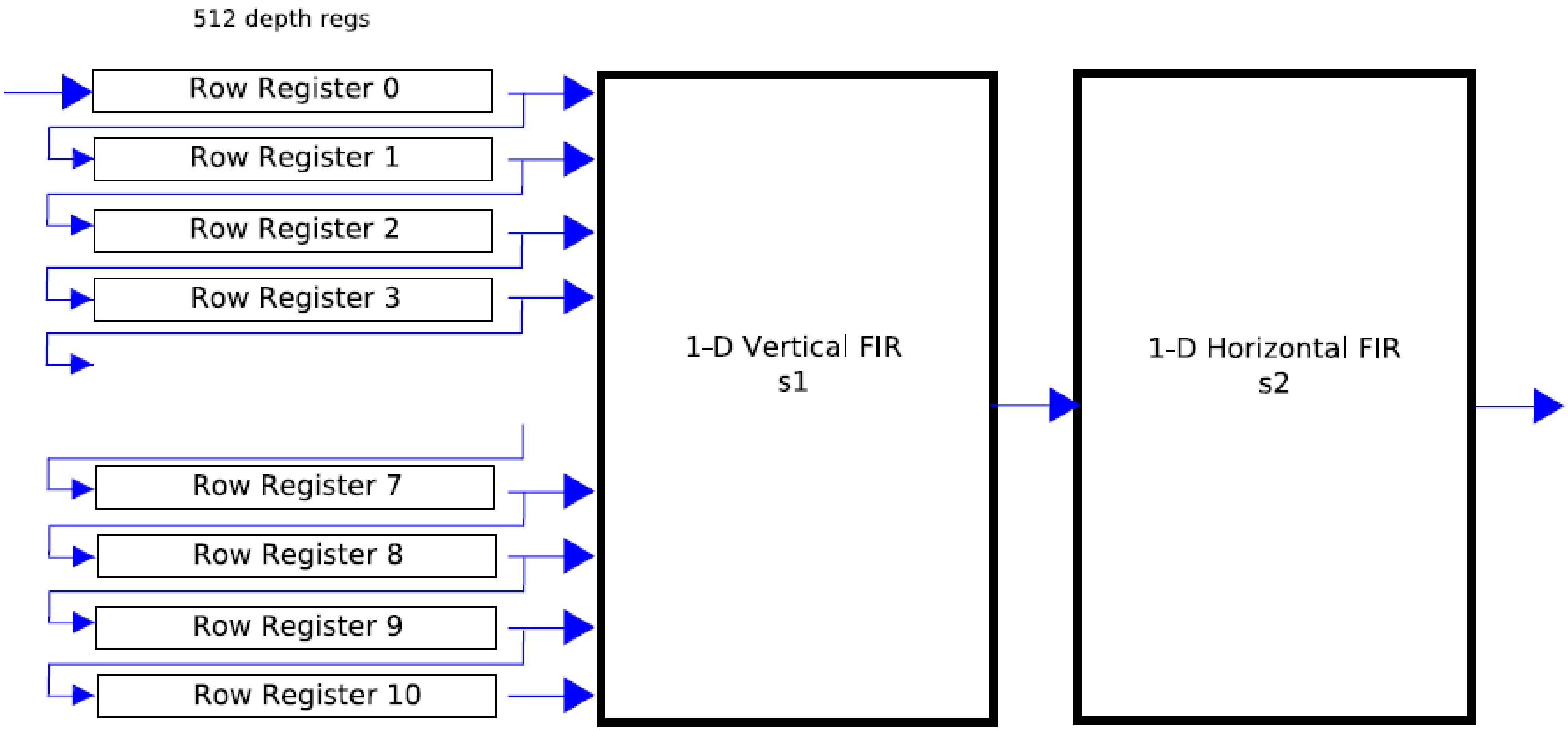

Vertical filter

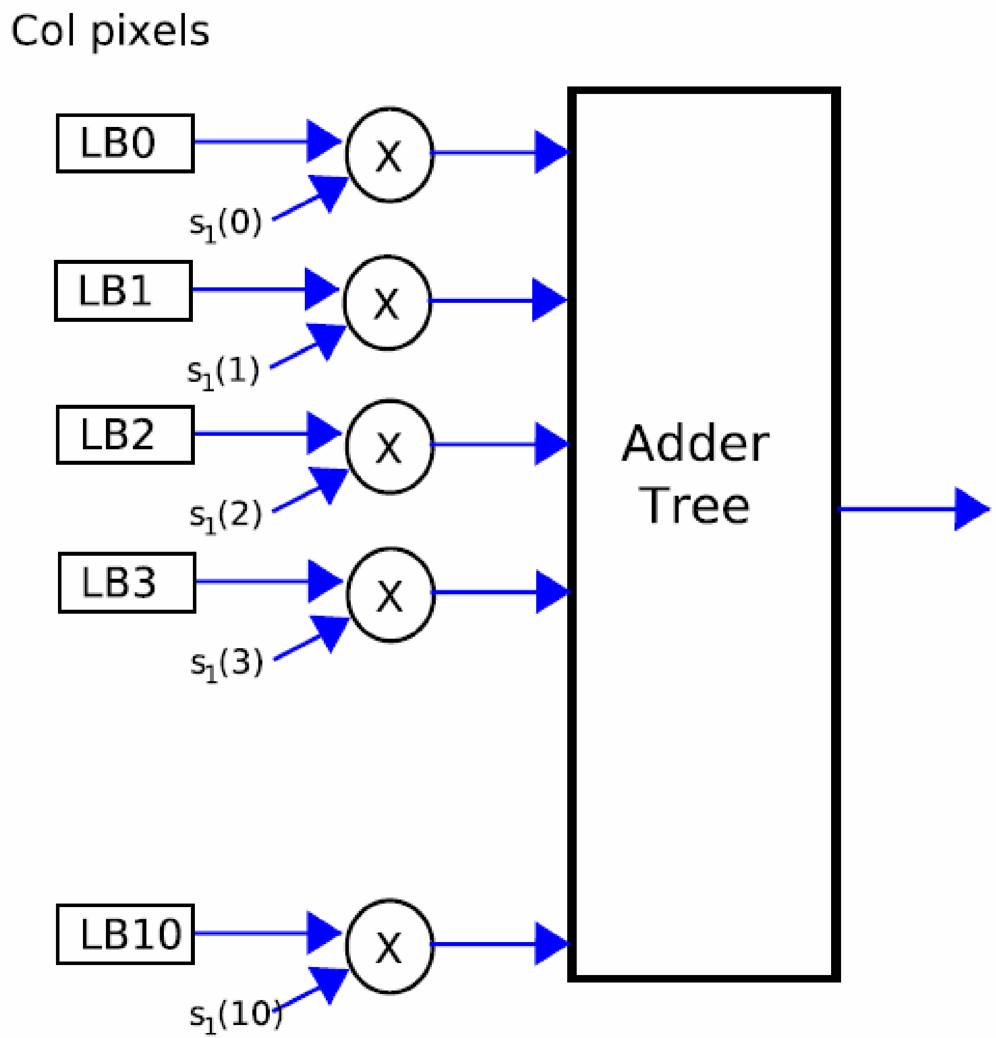

This 1D filter has kernel s_1 and multiplies all pixels in a column of 11 pixels by the kernel coefficients, followed by the adder tree that sums up the results two by two.

Horizontal filter

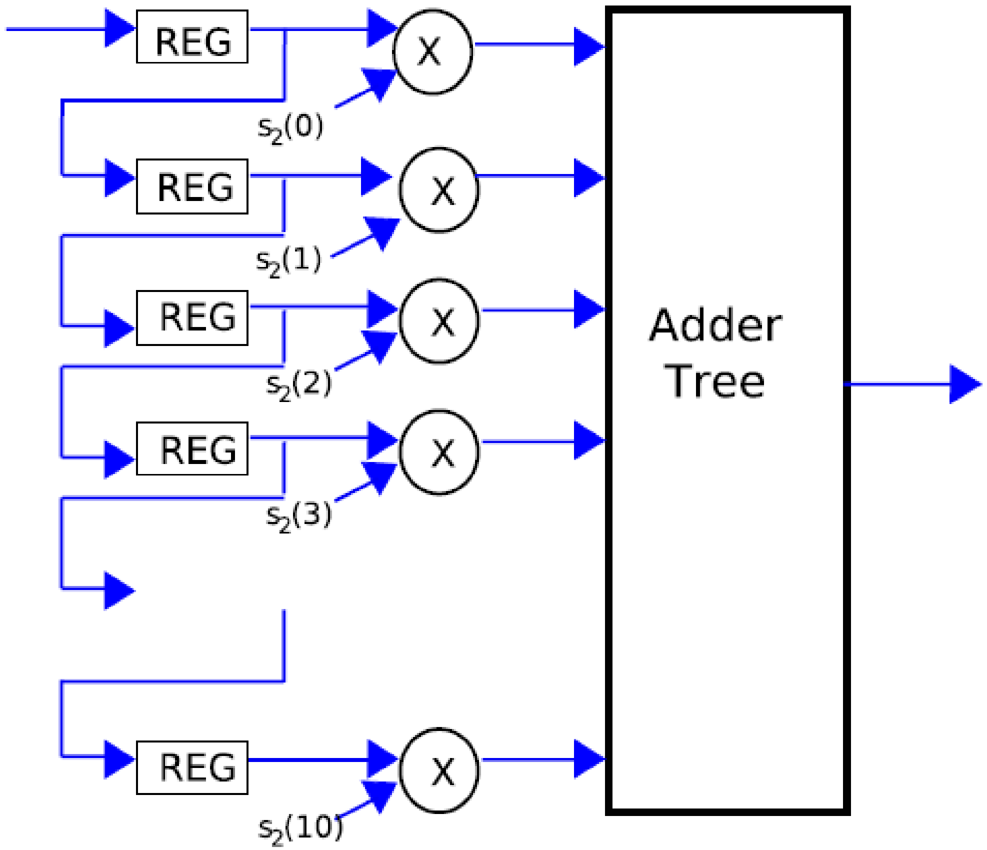

This 1D filter has kernel s_2 and its inputs are delayed and organized in rows through a series of cascaded registers that reconstruct the spatial dependence.

Selected references

Books

Principles of Optics: Electromagnetic Theory of Propagation, Interference and Diffraction of Light, 7th edition., Born, M. and Wolf, E., Cambridge University Press, Cambridge, United Kingdom, 952 pages (1999).

Video Microscopy (Methods in Cell Biology, 56)., Sluder, G. and Wolf, D. (eds), Academic Press, New York, 334 pages (1998).

Deconvolution of Images and Spectra, 2nd edition., Jansson, P. (ed), Academic Press, San Diego, California, 514 pages (1997).

Introduction to Fourier Optics., Goodman, J., McGraw-Hill, New York, 441 pages (1996).

Digital Image Processing: Principles and Applications., Baxes, G., John Wiley and Sons, New York, 452 pages (1994).

Digital Image Processing., Castleman, K., Prentice-Hall, Englewood Cliffs, New Jersey, 667 pages (1979).

Review Articles

Image-restoration methods: basics and algorithms., Boccacci, P. and Bertero, M., in ***Confocal and Two-Photon Microscopy: Foundations, Applications, and Advances***, Diaspro, A. (ed), Wiley-Liss, New York, pages 253-269 (2002).

A workingperson's guide to deconvolution in light microscopy., Wallace, W., Schaefer, L., and Swedlow, J., in ***BioTechniques, 31(5)***, pages 1076-1097 (2001).

Contrast, resolution, bleaching and statistics in confocal microscopy., Pawley, J., in ***Focus on Multidimensional Microscopy***, Cheng, P., Hwang, P., Wu, J., Wang, G., and Kim, H. (eds), World Scientific, Singapore, pages 134-141 (1999).

Three-dimensional imaging by deconvolution microscopy., McNally, J., Karpova, T., Cooper, J., and Conchello, J., in ***Methods, 19***, pages 373-385 (1999).

Computational deblurring of fluorescence microscope images., Shaw, P., in ***Cell Biology: A Handbook, 2nd edition***, Academic Press, San Diego, California, pages 206-217 (1998).

Confocal microscopy and deconvolution techniques., Spector, D., Goldman, R., and Leinwand, L., in ***Cells: A Laboratory Manual, Volume 2, Light Microscopy and Cell Structure***, Cold Spring Harbor Laboratory Press, Cold Spring Harbor, New York, pages 96.1-96.23 (1998).

High resolution 3-D imaging of living cells by image restoration., Carrington, W., Fogarty, K., Lifshitz, L., and Tuft, R., in ***Imaging Living Cells***, Rizzuto, R. and Fasolato, C. (eds), Springer-Verlag, Heidelberg, Germany, pages 30-50 (1998).